International Journal of Heat and Technology
Vol. 44, No. 2, April, 2026, pp. 767-776
Journal homepage: http://iieta.org/journals/ijht

Design and Numerical Evaluation of a Forced-Air Duct Cooling System for the Thermal Management of Brake Discs in a Heavy-Duty Van

Luis Farfán Medina, Cesar Torres Mollo, Yuri Silva Vidal, Mauricio Salazar Ccama, José Canazas*

Department of Mechanical Engineering, Universidad Nacional de San Agustín de Arequipa, Arequipa 04001, Peru

Corresponding Author Email: jcanazas@unsa.edu.pe

https://doi.org/10.18280/ijht.440227

Received: 5 February 2026
Revised: 11 April 2026
Accepted: 19 April 2026
Available online: 30 April 2026

Keywords:
computational fluid dynamics, brake cooling, heat transfer, brake disc, aerodynamics

ABSTRACT

Efficient thermal management of braking systems is essential to ensure vehicle safety and maintain braking performance under severe operating conditions. In this study, the aero-thermal behavior of a brake cooling duct and its influence on the convective heat transfer characteristics of a ventilated brake disc were investigated numerically using computational fluid dynamics (CFD). The simulations considered different inlet air flow velocities representing typical vehicle operating conditions, as well as three imposed surface temperatures for the brake disc: 600 K, 700 K, and 800 K. The results show that increasing the inlet air flow velocity significantly improves the duct's convective cooling capacity, reducing the air temperature within the flow domain by more than 100 K compared to the condition with the lowest velocity. However, this improvement is accompanied by higher aerodynamic losses due to the increase in pressure drop along the duct. It was observed that the spatial distribution of the wall heat transfer coefficient over the disc surface is primarily controlled by the local airflow structure, with typical values ranging from 90 to 140 W m^{-2} K^{-1} and maximum values reaching approximately 180 W m^{-2} K^{-1} near the ventilation ducts. The brake disc was modeled as stationary; therefore, the reported cooling performance may be conservative, as rotational effects that enhance internal airflow were not considered.

1. INTRODUCTION

Efficient thermal management of braking systems remains a critical challenge in heavy-duty commercial vans operating under sustained load conditions [1]. During braking, a substantial portion of the vehicle's kinetic energy is converted into thermal energy at the pad-disc interface [2]. During repeated or prolonged braking, such as extended driving on downhill slopes, high-frequency urban traffic, or fully loaded transport, this heat accumulates in the brake disc, generating high surface temperatures and significant thermal gradients [3, 4]. If heat dissipation is insufficient, the resulting thermal stress can lead to brake fade, reduced coefficient of friction, accelerated wear, surface cracking, and permanent deformation of the disc, ultimately compromising braking reliability and vehicle safety [5].

Commercial vans have a different operating profile than high-performance or racing vehicles. Instead of short-duration extreme braking, these platforms are subjected to sustained thermal loading under high gross weights and variable maneuvering conditions [6]. While ventilated discs promote internal airflow and improve heat transfer by convection, their effectiveness depends largely on the availability and directionality of external airflow within the wheel well. In practical driving situations, airflow distribution around the brake assembly is often irregular and can be significantly affected by vehicle speed, underbody flow structures, and steering-induced geometric variations [7, 8].

Traditional strategies to mitigate brake overheating include increasing the disc mass, modifying the internal ventilation geometry, or using high-temperature-resistant materials [9, 10]. While these approaches improve thermal capacity, they do not directly address the external mechanism of convective heat transfer that regulates heat dissipation during vehicle motion. A more direct strategy involves channeling high-pressure frontal airflow toward the brake assembly through dedicated ducting systems, thereby increasing local air velocity and convective heat dissipation at the disc surface [11].

Air duct cooling systems are commonly implemented in motorsports applications, where aerodynamic optimization and design flexibility facilitate their integration [12]. However, heavy-duty commercial vans operate under very different aerodynamic constraints and space limitations. The integration of a forced-air duct into these platforms must account for underbody flow behavior, wheel well confinement, steering angle variability, suspension movement, and pressure losses along the duct path [13]. Despite the practical relevance of these vehicles in logistics, emergency services, and passenger transport, research on the integrated aero-thermal performance of brake cooling duct systems specifically designed for commercial van geometries has been limited. In particular, the combined influence of variations in inlet velocity and steering angle on airflow distribution and

cooling efficiency within the wheel assembly remains insufficiently explored [1, 14].

Recent studies have explored various strategies for improving the thermal performance of braking systems using numerical and experimental approaches. CFD-based research has focused primarily on optimizing the geometries of ventilated discs and their influence on internal airflow structures and heat dissipation, demonstrating that geometric modifications can significantly improve convective cooling performance [9, 15]. Complementarily, coupled aerothermal simulations have been used to evaluate the interaction between flow fields and temperature distribution under different operating conditions, highlighting the importance of accurately capturing airflow behavior to predict thermal response [10, 16, 17]. In parallel, experimental studies have examined the relationship between mass flow rate through ventilated discs and cooling efficiency, confirming that the intensity and distribution of the airflow are critical parameters governing heat removal [18]. Despite these advances, existing research has focused primarily on analysis at the rotor level or on isolated configurations, paying little attention to the complete path of the airflow from the external inlet zones to the brake assembly. In particular, the combined effects of varying inlet velocity and direction-induced geometric changes in airflow distribution within the wheel housing remain insufficiently addressed, especially in the context of heavy-duty commercial vehicle platforms.

In this context, the present study proposes the design and numerical evaluation of a forced-air duct cooling system dedicated to the thermal management of brake discs in a heavy-duty van. The system captures airflow from the lower front area of the vehicle, independent of the radiator core, and channels it through a dedicated duct toward the brake assembly. The numerical analysis evaluates the aerothermal performance of the configuration under different inlet velocities representative of realistic driving scenarios, also considering variations in the steering angle to assess the geometric effects on the wheel well. This study is limited to evaluating the performance of a forced-air duct cooling system for brake discs under different inlet velocities and steering conditions representative of real-world vehicle scenarios.

2. METHODOLOGY

2.1 Description of the brake line and brake disc

This study investigates the aerothermal performance of a forced-air duct system designed to improve the cooling of a brake disc in a heavy-duty commercial van. The methodology is based on a two-step numerical approach: first, the airflow behavior within the duct is analyzed independently, followed by an evaluation of the brake disc's thermal response. Figure 1 shows a schematic of the duct and the brake assembly with the suspension system.

The principal geometric parameters of the brake cooling duct and brake disc considered in the numerical model are summarized in Tables 1 and 2, respectively. These dimensions were selected to represent a generic heavy-duty commercial vehicle brake cooling configuration while maintaining realistic spatial relationships between the duct outlet and the brake assembly.

The proposed duct system is located in the lower front region of the vehicle, below the radiator inlet, allowing incoming air to be drawn in without interfering with the engine's main cooling system. The duct's geometry consists of an inlet section with a relatively large cross-sectional area, followed by a curved channel that guides the airflow toward the brake assembly. The cross-section gradually adapts along its length to accommodate spatial constraints and maintain flow continuity until reaching the outlet region near the brake disc.

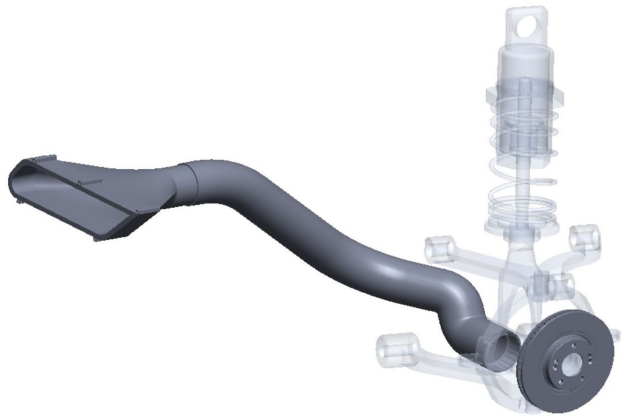

Figure 1. Schematic of the duct and brake assembly with the suspension system

Table 1. Duct geometry

Parameter	Value
Total duct length	858 mm
Inlet cross-sectional area	0.023175 m^2
Outlet cross-sectional area	0.005254 m^2
Hydraulic diameter at inlet	113.46 mm
Hydraulic diameter at outlet	81.8 mm
Main curvature radius	70 mm

Table 2. Brake disc geometry

Parameter	Value
Outer disc diameter	106.5 mm
Inner disc diameter	65.53 mm
Disc thickness	19 mm
Ventilation channel width	9.8 mm

The brake system considered in this study corresponds to a conventional disc configuration, typical in commercial vans. The disc is modeled as a solid component with defined thermal boundary conditions representing heat generation during braking. Although the exact vehicle geometry is not fully reproduced, the relative position between the duct outlet and the brake disc is maintained to ensure realistic interaction between the airflow and the braking surface. The duct configuration proposed in this study is intended to be generic and not linked to a specific heavy-duty van model. Therefore, the analysis focuses on fundamental aerothermal behavior under representative operating conditions rather than on a particular vehicle geometry.

To account for real-world driving conditions, three different relative positions between the duct outlet and the brake disc are considered. These configurations simulate: (i) a neutral position where the airflow is approximately orthogonal to the disc surface, and (ii) two additional positions representing left- and right-turn conditions at 30 degrees, which alter the alignment between the incoming airflow and the brake

assembly.

2.2 Numerical simulation

The numerical analysis was performed using computational fluid dynamics (CFD). The simulations were carried out using ANSYS CFX software, employing a three-dimensional steady-state formulation to investigate the aerodynamic and thermal behavior of the duct and the brake disc. The flow was assumed to be incompressible, as the Mach number is less than 0.3, and turbulent. Air thermophysical properties were assumed constant throughout the simulations in order to simplify the numerical analysis and isolate the influence of airflow structure and inlet velocity on the convective cooling behavior of the brake system.

The equations governing the flow correspond to the conservation of mass, momentum, and energy, which were solved within the software. The effects of turbulence were modeled using an SST k-omega model.

Two independent computational domains were defined. The first domain corresponds to the airflow through the duct, with the objective of determining the velocity distribution, pressure drop, and temperature of the outlet air. The second domain represents the brake disc, where the thermal response under forced convection conditions is evaluated.

For the duct simulation, three inlet velocities were imposed to represent different vehicle operating conditions: 30 km/h, 60 km/h, and 90 km/h. A uniform velocity profile was specified at the inlet, while an outlet pressure condition was applied at the duct outlet. All solid surfaces were treated with no-slip boundary conditions. Two heat flux boundary conditions were considered for the duct, since it is located near the vehicle's combustion engine; in the area closest to the engine, a heat flux of 10,000 W/m² was assumed, and due to the vehicle's own heating, a heat flux of 4,000 W/m² was assumed for the rest of the duct.

In the brake disc simulations, the inlet airflow conditions were defined based on the results obtained from the duct analysis. Three different temperature values were applied to the disc surface: 600 K, 700 K, and 800 K, to represent different braking intensities. Therefore, the present analysis focuses on the convective cooling characteristics and heat transfer behavior of the system rather than on the transient thermal response of the brake disc itself. In addition, three relative positions between the duct outlet and the brake disc were considered, corresponding to the neutral alignment and left- and right-turn conditions, respectively. For the present study, the rotation of the brake disc is not considered. This simplification allows the analysis to isolate the effect of the externally forced airflow provided by the duct on the thermal behavior of the brake system. However, it is acknowledged that in real operating conditions, disc rotation induces a centrifugal pumping effect within the ventilation channels, which enhances internal airflow and convective heat transfer. Therefore, the present approach may underestimate the absolute cooling performance of the brake disc.

2.3 Mesh convergence analysis

A mesh independence study was conducted to ensure the reliability and accuracy of the numerical results. The computational domains for the brake duct and brake disc simulations were discretized using tetrahedral element meshes. Various mesh densities were generated and evaluated for each domain. During the refinement process, key output parameters were monitored, as well as the average surface temperature of the brake disc.

The mesh was progressively refined until the variation in the monitored parameters between successive mesh levels remained within a low acceptable threshold. Table 3 shows the mesh independence analysis for the duct, considering an air inlet velocity of 60 km/h. Three parameters were considered in this case: the outlet velocity, the pressure drop, and the outlet temperature. It was observed that all values had a difference of less than 0.1%, so it was decided to use a mesh of 600,000 elements for the simulations at the other velocities

Table 4 shows the mesh independence analysis for the brake disc, assuming a disc surface temperature of 600 K and an outlet velocity of 75 km/h from the duct, as shown in Table 4. For this case, two analysis parameters were considered: the convective heat transfer coefficient and the total dissipated power. Thus, it can be observed that the differences again amount to values less than 0.1%, so it is decided to use a mesh of approximately 750,000 elements for simulations with the brake disc in other positions and at different surface temperatures.

Table 3. Assessment of the pipeline's mesh independence at 60 km/h

Elements	Velocity Outlet (m/s)	Difference (%)	Pressure Drop (Pa)	Difference (%)	Temperature Outlet (K)	Difference (%)
251452	75.7594	-	4537.3343	-	302.740	-
322147	75.4817	0.3679	4542.1126	0.1052	302.810	0.0231
408951	75.2751	0.2745	4547.8426	0.1260	302.860	0.0165
499852	75.1206	0.2057	4555.5421	0.1690	302.850	0.0033
601587	75.0697	0.0678	4560.0498	0.0988	302.848	0.0006
704658	75.0321	0.0501	4562.0175	0.0431	302.847	0.0003

Table 4. Evaluation of the brake disc's mesh independence at a surface temperature of 600 K

Elements	Convective Heat Transfer Coefficient (W/m^2-K)	Difference (%)	Total Power Dissipation (W)	Difference (%)
217247	99.380	-	4030.65	-
319546	94.254	5.4385	4070.17	0.9710
404378	91.169	3.3843	4108.91	0.9428
511265	90.853	0.3474	4092.14	0.4098
643785	90.652	0.2217	4084.35	0.1907
780502	90.539	0.1247	4082.28	0.0507
902457	90.512	0.0303	4081.34	0.0230

Table 5. Evaluation of the brake disc's mesh independence at the inner top of the brake disc

Elements	Wall Heat Flux (W/m^2)	Difference (%)	Surface Temperature (K)	Difference (%)
217247	1714.235	-	373.234	-
319546	1650.851	3.8395	364.981	2.2612
404378	1608.904	2.6071	357.304	2.1486
511265	1587.060	1.3764	353.005	1.2178
643785	1580.742	0.3997	350.127	0.8219
780502	1577.621	0.1978	348.521	0.3658
902457	1576.348	0.0808	348.522	0.0944

The results presented in Tables 3 and 4 indicate that both components achieve mesh-independent convergence at these levels of discretization; therefore, using a mesh with more than 600,000 and 750,000 elements, respectively, represents an appropriate trade-off between numerical accuracy and computational cost. This step is essential to ensure that the differences observed between the duct configurations are due to geometric conditions and not to errors caused by insufficient mesh resolution.

In addition to the global parameters presented above, a local mesh sensitivity analysis was carried out to ensure that the numerical solution accurately captures spatial variations in the thermal field. For this purpose, local values of wall heat flux and air-side surface temperature were monitored on the inner top of the brake disc where air enters directly into the disc. The results of this analysis are presented in Table 5. It can be observed that the variation of these local quantities between successive mesh refinements remains within a small acceptable range, indicating that the mesh is sufficiently fine to resolve local gradients in both flow and heat transfer. This confirms that the selected mesh provides grid-independent results not only for global performance indicators but also for localized thermal behavior.

3. RESULTS

This section presents the numerical results obtained from CFD simulations of the brake cooling duct and the associated aerothermal behavior of the brake disc. The analysis focuses on three main aspects of cooling performance. First, the influence of the inlet air velocity on the internal flow structure and the thermal behavior of the duct is examined. Second, the resulting pressure losses and aerodynamic characteristics are evaluated to determine the impact of airflow acceleration within the duct geometry. Finally, the convective heat transfer performance at the brake disc surface is analyzed using the spatial distributions of the wall heat transfer coefficient and wall heat flux under different imposed disc temperatures. Taken together, these results provide a comprehensive understanding of the interaction between airflow dynamics and the heat transfer mechanisms that govern the cooling performance of the proposed duct configuration.

3.1 Effect of the inlet velocity into the duct

The inlet air velocity is one of the key parameters governing the aerodynamic and thermal performance of the proposed brake cooling duct. Figures 2 and 3 show the temperature and absolute pressure distributions inside the duct for three representative vehicle speeds: 30 km/h, 60 km/h, and 90 km/h. These results allow us to evaluate how variations in the inlet airflow affect both convective heat transfer within the duct and the associated aerodynamic losses.

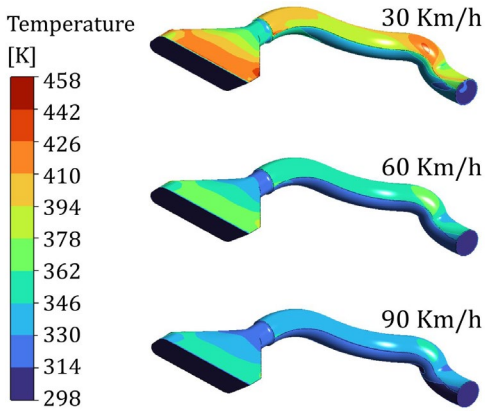

Figure 2. Temperature distribution in the duct for three air inlet speeds: 30, 60, and 90 km/h

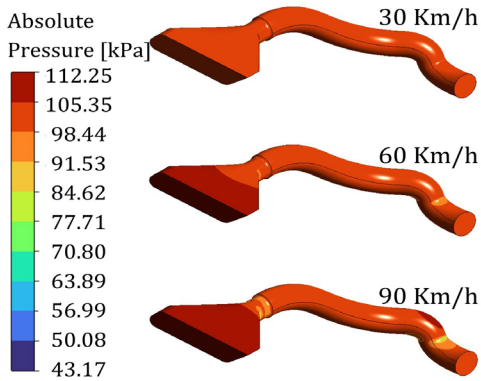

Figure 3. Absolute pressure distribution in the duct for three air inlet velocities: 30, 60, and 90 km/h

The temperature distribution within the duct shows a strong dependence on the inlet velocity. At the lowest speed (30 km/h), the airflow undergoes significant heating as it moves through the duct due to the heat flux imposed on the duct walls. Under these conditions, air temperatures exceed 430 K near the inlet and remain above approximately 380 K over much of the duct's length. This behavior indicates a limited ability of the flow to remove heat from the surrounding surfaces, primarily due to the relatively low kinetic energy of the incoming air. The reduced velocity causes a thicker thermal boundary layer to form along the duct walls, which decreases the local temperature gradient at the wall and, consequently, reduces the convective heat transfer coefficient. In addition, the curved sections of the duct promote flow separation and localized recirculation, which increases the residence time of the hot air and further contributes to the high temperatures observed inside the duct.

A significant improvement in thermal performance is observed when the inlet velocity is increased to 60 km/h. In this configuration, the air temperature inside the duct

decreases considerably, reaching temperatures between 330 and 370 K over most of the flow domain. Compared to the 30 km/h case, this represents a temperature reduction of between 50 and 70 K in large areas of the duct. The improvement is primarily associated with convective transport intensified by the higher air flow velocity. As the Reynolds number increases, the boundary layer thickness decreases, and the intensity of turbulence near the walls increases, which raises the local heat transfer coefficient and facilitates more efficient heat dissipation from the duct surfaces. Furthermore, the increased flow momentum reduces the extent of recirculation zones along the curved sections of the duct, promoting a more attached flow and a more uniform thermal field throughout the duct.

The highest inlet velocity considered in this study (90 km/h) produces the most favorable thermal behavior. Under these conditions, the air temperature remains near 300–320 K throughout most of the duct, indicating that the airflow is capable of effectively removing the heat load imposed on the duct walls. Compared to the 30 km/h case, the average air temperature inside the duct decreases by more than 100 K, demonstrating the strong influence of the inlet velocity on the system's convective cooling capacity. It should be noted that this temperature reduction corresponds to the airflow temperature within the duct and does not represent a direct reduction in the brake disc surface temperature. In the present study, the disc temperature was prescribed as a boundary condition to evaluate the convective heat transfer behavior under different airflow conditions. The increase in flow velocity intensifies the convective heat transfer mechanism by reducing the thickness of the thermal boundary layer and increasing turbulent mixing within the flow. Furthermore, the increased momentum of the airflow shortens the residence time of the air within the duct, limiting the amount of heat absorbed by the fluid as it moves toward the outlet.

While higher inlet velocities significantly improve the duct's thermal performance, they also introduce greater aerodynamic losses. The pressure distributions shown in Figure 3 indicate that the pressure drop along the duct increases progressively with inlet velocity. For the 30 km/h condition, the pressure gradient along the duct is relatively gentle, indicating relatively small aerodynamic losses associated with wall friction and geometric changes in the duct cross-section. However, as the inlet velocity increases to 60 km/h, the pressure drop increases substantially, reaching values close to 4.5–4.6 kPa between the inlet and outlet sections.

At maximum speed (90 km/h), pressure losses increase even further due to the quadratic relationship between dynamic pressure and flow velocity. The greater inertial forces associated with higher speeds amplify both the friction losses at the duct walls and the local losses generated by the curvature and cross-sectional transitions. The pressure field also reveals localized regions of high pressure near the inlet, where the airflow initially decelerates upon entering the duct, followed by a gradual reduction in pressure in the flow direction as the air accelerates through the curved channel.

These results highlight a clear trade-off between thermal performance and aerodynamic efficiency. Increasing the inlet velocity significantly improves the duct's convective heat dissipation capacity, reducing the air temperature within the system and enhancing the cooling potential of the airflow supplied to the brake assembly. However, this improvement leads to higher pressure losses, which can affect the vehicle's overall aerodynamic efficiency and the airflow available for cooling. Therefore, the duct's optimal operating condition must balance these opposing effects to maximize cooling efficiency and minimize the associated aerodynamic penalty.

It should be noted that the pressure losses reported in the present study correspond primarily to internal aerodynamic losses within the brake cooling duct itself. The proposed duct configuration is positioned below the main radiator inlet and was designed to operate independently from the primary engine cooling airflow. Therefore, the predicted pressure drop is not expected to significantly affect the intake airflow supplied to other thermal management components such as the radiator, intercooler, or oil cooler. Nevertheless, the increase in pressure losses at higher vehicle speeds may contribute to a localized aerodynamic penalty and slightly influence the overall underbody airflow behavior of the vehicle. From an engineering perspective, this highlights the importance of optimizing the duct geometry in order to balance enhanced brake cooling performance with acceptable aerodynamic efficiency. Minimizing unnecessary flow resistance and reducing localized losses within the duct may improve cooling effectiveness while limiting potential impacts on overall vehicle aerodynamic performance.

3.2 Effect of the brake disc position

Figure 4 presents the airflow streamlines colored by velocity magnitude around the brake cooling duct and brake disc for different steering configurations. The flow field reveals the formation of accelerated jet-like regions at the duct outlet, together with recirculation structures and localized vortical motion around the brake assembly. These flow features strongly influence the spatial distribution of the convective heat transfer coefficient observed on the disc surface.

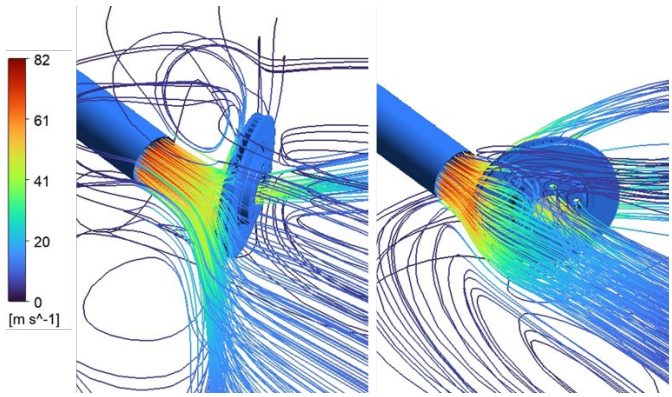

Figure 4. Airflow streamlines colored by velocity magnitude around the brake cooling duct and brake disc for different steering positions

Regions directly exposed to the accelerated airflow exhibit higher local velocities and enhanced turbulent mixing, which promote thinner thermal boundary layers and consequently higher convective heat transfer coefficients. In contrast, areas affected by flow separation and recirculation exhibit lower local momentum and reduced cooling effectiveness. The streamline distributions also show that changes in the relative alignment between the duct outlet and the brake disc modify the trajectory and impingement location of the incoming airflow, thereby affecting the local heat transfer behavior across the disc surface.

The relative orientation between the brake disc and the outlet of the forced-air duct significantly affects the aerodynamic interaction between the cooling airflow and the rotor surface. Figures 5 and 6 show the distributions of the convective heat transfer coefficient at the wall and the corresponding heat flux for three steering configurations: straight alignment and two steering positions corresponding to a 30° rotation of the wheel to the left and to the right.

The convective heat transfer coefficient shown in Figure 5 exhibits clear differences in both magnitude and spatial distribution depending on the disk's orientation. In the straight configuration, the airflow emerging from the duct strikes the rotor relatively symmetrically, producing a moderately uniform heat transfer distribution across the disk's surface. Most of the rotor area is characterized by heat transfer coefficient values ranging approximately between 90 and 150 W m^{-2} K^{-1}, while regions located near the outer edge reach values exceeding 200 W m^{-2} K^{-1} due to flow acceleration and increased turbulence intensity. The spatially averaged convection coefficient over the rotor surface is estimated to be on the order of 120–140 W m^{-2} K^{-1}, indicating stable but moderate cooling performance.

When the wheel rotates 30° to the left, the alignment between the airflow and the disk surface becomes less favorable. In this configuration, the incident jet interacts with the rotor at a more oblique angle, which reduces the effective momentum transfer to certain parts of the disk surface. Consequently, the distribution of the convective heat transfer coefficient becomes more heterogeneous. While maximum values close to 200–240 W m^{-2} K^{-1} are still observed in regions directly exposed to the incident airflow, larger areas of the rotor remain within the lower range of 80–130 W m^{-2} K^{-1}. This results in a slightly lower average surface heat transfer coefficient compared to the straight configuration, suggesting a modest degradation in cooling efficiency.

In contrast, the 30° right-hand configuration provides the most favorable aerodynamic alignment between the duct outlet and the brake disc. Under these conditions, the airflow strikes the rotor surface more directly, increasing the magnitude of the local velocity and intensifying turbulence levels in the near-wall region. This interaction generates a broader distribution of high convective coefficients, with significant portions of the disc surface exhibiting values between 140 and 220 W m^{-2} K^{-1}, and local maxima approaching 350–380 W m^{-2} K^{-1} near the outer radius. Consequently, the spatially averaged heat transfer coefficient in this configuration is significantly higher than in the other two cases, indicating a more efficient convective cooling process.

The influence of the disk orientation on cooling performance is further confirmed by the wall heat flux distributions shown in Figure 6. Since the heat flux at the wall is governed by the relationship between the convective heat transfer coefficient and the difference between the surface and ambient temperatures, the observed variations in the convective heat transfer coefficient are directly reflected in the heat flux patterns. In the straight configuration, most of the rotor surface exhibits heat flux values between approximately 2 and 4 kW m^{-2}, with localized peaks reaching 6–7 kW m^{-2} near the outer perimeter.

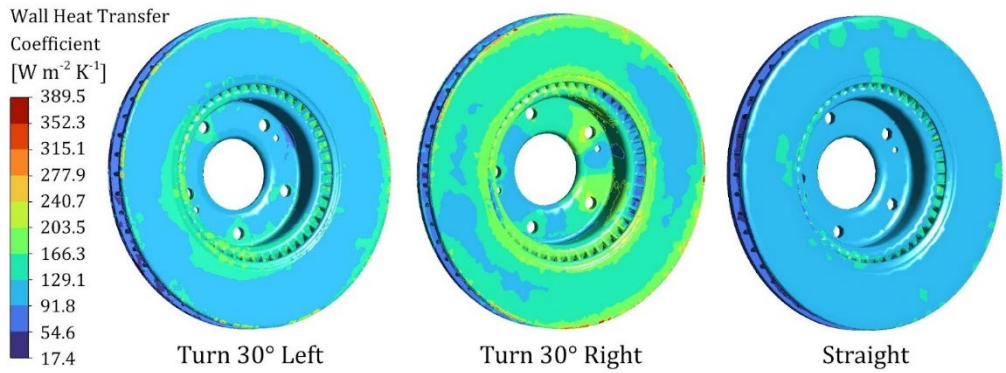

Figure 5. Distribution of the heat transfer coefficient on the wall along the brake disc, considering three positions of the disc relative to the vehicle: turned 30 degrees to the left, turned 30 degrees to the right, and facing forward

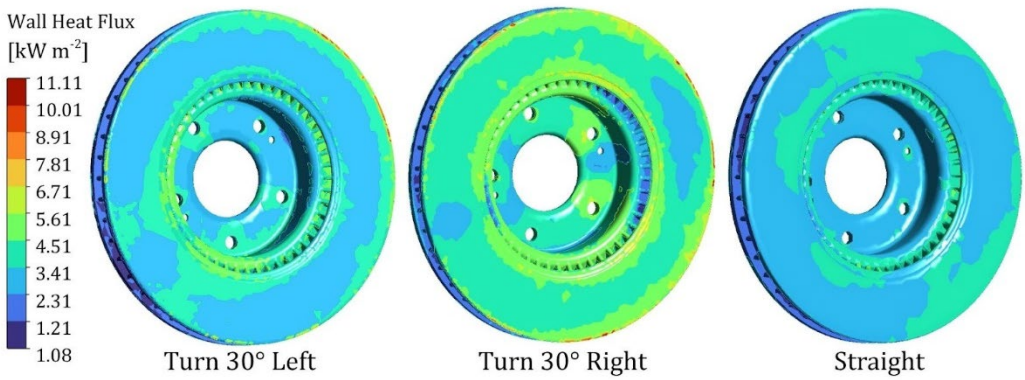

Figure 6. Heat flux distribution across the brake disc, considering three positions of the disc relative to the vehicle: turned 30 degrees to the left, turned 30 degrees to the right, and facing forward

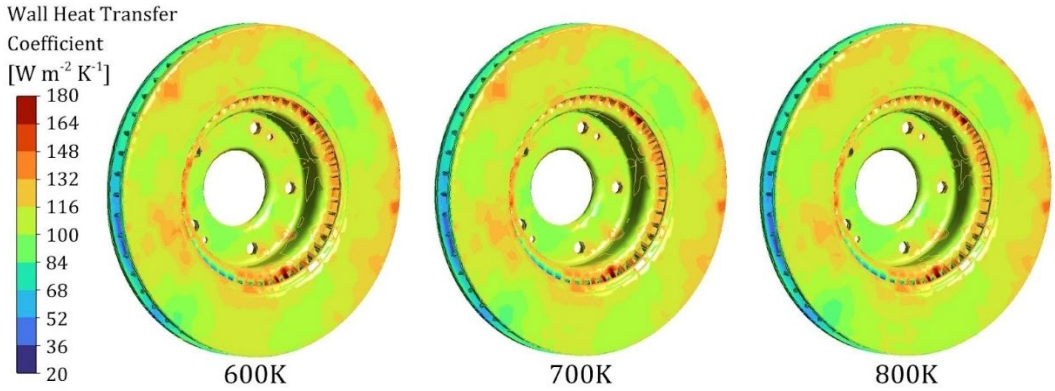

Figure 7. Distribution of the heat transfer coefficient in the wall along the brake disc, considering three disc surface temperatures: 600 K, 700 K, and 800 K

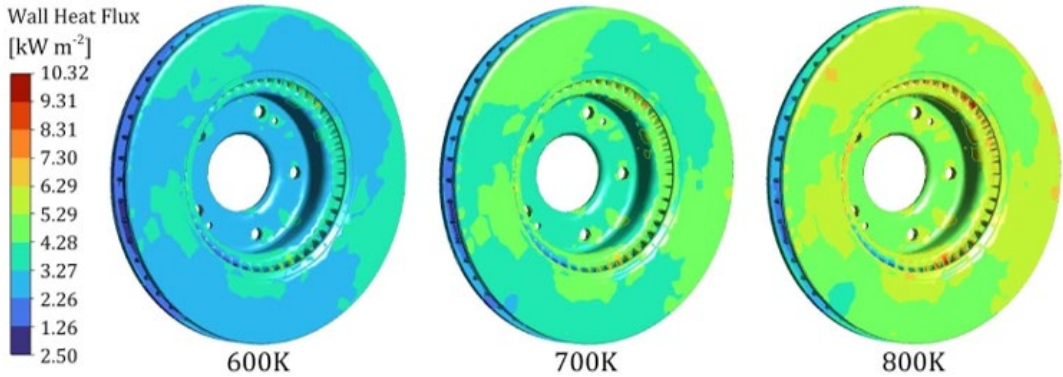

Figure 8. Heat flux distribution in the wall along the brake disc, considering three disc surface temperatures: 600 K, 700 K, and 800 K

In the left-hand configuration, the heat flux distribution becomes more irregular due to the asymmetric interaction between the incident airflow and the rotor surface. Regions directly exposed to the flow maintain relatively high heat dissipation rates, while areas affected by partial aerodynamic shielding show reduced heat flux values, close to 2-3 kW m^{-2}. This confirms that the altered flow orientation limits the overall effectiveness of the convective cooling mechanism.

On the other hand, the right-hand configuration produces the highest heat dissipation levels across the entire rotor. Large areas of the disk exhibit heat flux values between 4 and 7 kW m^{-2}, with localized maxima approaching 10–11 kW m^{-2} near the outer radius. This represents the most effective cooling scenario among the three configurations, as a result of the greater flow impact and the greater disturbance of the boundary layer.

In summary, the results demonstrate that steering-induced variations in the relative alignment between the duct outlet and the brake disc can significantly influence the system's convective cooling performance. The 30° right-hand steering position provides the most favorable aerodynamic interaction, resulting in higher average heat transfer coefficients and greater heat dissipation rates. Conversely, the left-hand steering configuration slightly reduces cooling efficiency due to the less-than-optimal alignment of the airflow with the rotor surface. These findings highlight the importance of considering the effects of wheel articulation during the design of forced-air brake cooling systems, particularly in commercial vehicles where steering angles during operation can alter the local flow field within the wheel assembly.

3.3 Effect of brake disc surface temperature

Figures 7 and 8 show the spatial distribution of the heat transfer coefficient at the wall and the heat flux on the surface of the brake disc for three specified temperatures: 600 K, 700 K, and 800 K. These results provide insight into how the thermal driving force and the aerodynamic field within the duct influence the convective heat dissipation of the brake disc.

The distribution of the wall heat transfer coefficient, shown in Figure 6, exhibits relatively similar spatial patterns for all three temperatures. Most of the disc surface exhibits values in the range of approximately 90–140 W m^{-2} K^{-1}, while regions located near the internal ventilation channels reach values close to 160–180 W m^{-2} K^{-1}. These higher coefficients are observed primarily along the inner annular region of the disc, where the airflow accelerates through the ventilation ducts. The increase in velocity in these regions intensifies turbulent mixing and reduces the thickness of the thermal boundary layer, resulting in higher local convective heat transfer coefficients.

In contrast, lower heat transfer coefficients—typically less than 60 W m^{-2} K^{-1}—are observed near the outer edge of the disk and in regions where the airflow velocity decreases due to flow expansion or recirculation. These areas correspond to zones where the local flow momentum is reduced, resulting in thicker boundary layers and, consequently, weaker convective heat transfer. The general similarity in the heat transfer coefficient distributions for the three temperature conditions indicates that the convective heat transfer coefficient is determined primarily by the flow dynamics within the cooling

duct, rather than by the absolute temperature of the disk surface. It should be noted that the present simulations assume constant air thermophysical properties. Under real operating conditions, variations in air viscosity and thermal conductivity at elevated temperatures may slightly modify the local convective heat transfer coefficient. However, within the range of operating conditions considered in this study, the spatial distribution of the heat transfer coefficient remains governed primarily by the airflow structure, turbulence intensity, and local velocity distribution generated by the duct configuration. Therefore, the relatively small variation observed in the convective heat transfer coefficient between the different disc temperatures is considered physically consistent with the assumptions adopted in the numerical model.

While the spatial distribution of the heat transfer coefficient remains relatively constant, the heat flux at the wall, illustrated in Figure 8, shows a clear increase with disc temperature. For the 600 K case, most regions of the disk exhibit heat flux values between approximately 2.5 and 4.5 kW m^{-2}, with localized peaks reaching around 6-7 kW m^{-2} near the internal ventilation ducts. When the disc temperature increases to 700 K, the heat flux increases significantly across the entire surface, with typical values ranging between 4 and 7 kW m^{-2}, and maximum values approaching 8-9 kW m^{-2} in the same high-velocity regions.

The highest thermal condition, corresponding to a disk temperature of 800 K, produces the highest heat transfer rates. Under these conditions, the heat flux at the wall across significant portions of the disk surface exceeds 6 kW m^{-2}, while regions located near the ventilation channels reach values close to 10 kW m^{-2}. Compared to the 600 K case, this represents an increase in heat flux of approximately 60–80%, reflecting the greater thermal driving force between the heated disc surface and the incoming cooling airflow.

This behavior can be explained by the classical convective heat transfer equation, considering the convective heat transfer coefficient, the disk surface temperature, and the incoming air temperature. Since the heat transfer coefficient remains relatively stable under different thermal conditions, the increase in heat flux is primarily due to the greater temperature difference between the disc surface and the cooling air as the disc temperature rises.

Another important observation is the non-uniform distribution of heat flux across the disc surface. The highest heat transfer rates occur near the internal ventilation ducts, where the airflow accelerates and turbulence increases. These flow structures promote more intense convective heat exchange and enhance the system's local cooling capacity. In contrast, the outer regions of the disc experience lower heat transfer rates due to weaker interaction with the airflow and lower local velocities.

From a thermal management perspective, these results indicate that the cooling performance of the brake system is strongly influenced by the aerodynamic distribution of the airflow provided by the cooling duct. Areas exposed to higher-velocity flow benefit from significantly improved convective heat transfer, while areas with weaker airflow may experience reduced cooling efficiency. Therefore, optimizing the distribution of airflow within the duct and across the brake disc surface is essential for achieving a more uniform thermal field and preventing localized overheating during hard braking.

To assess the validity of the predicted convective heat transfer coefficients, the obtained values were compared with those reported in the literature for ventilated brake discs. Previous experimental and numerical studies have shown that the convective heat transfer coefficient on brake disc surfaces strongly depends on airflow conditions, disc geometry, and rotational effects. For instance, studies on ventilated brake discs have reported convective heat transfer coefficients in a similar order of magnitude, with values typically increasing with Reynolds number and airflow intensity [19, 20]. In addition, CFD investigations validated against experimental data have demonstrated good agreement between predicted and measured heat transfer coefficients for brake discs under realistic operating conditions [21]. Therefore, the range of 90-140 W m^{-2} K^{-1} obtained in the present study is consistent with previously reported values for forced convection over brake disc surfaces, supporting the physical reliability of the numerical model.

4. CONCLUSIONS

This study numerically investigated the aerodynamic and thermal performance of a forced-air brake cooling duct and its influence on the convective heat transfer characteristics of a ventilated brake disc using CFD. The results demonstrate that the inlet airflow velocity plays a critical role in the thermal behavior of the cooling system. Increasing the inlet velocity significantly improves the convective cooling capacity of the duct, reducing the air temperature inside the flow domain while enhancing turbulent mixing and decreasing the thermal boundary layer thickness along the duct walls. However, the improved cooling performance is accompanied by greater aerodynamic losses, reflected by the increase in pressure drop along the duct.

The numerical analysis further shows that the spatial distribution of the convective heat transfer coefficient on the brake disc surface is governed primarily by the local airflow structure generated by the duct configuration and the relative alignment between the airflow and the brake assembly. Most regions of the disc exhibit heat transfer coefficients between approximately 90 and 140 W m^{-2} K^{-1}, while areas near the internal ventilation channels reach values close to 180 W m^{-2} K^{-1} due to locally accelerated airflow and higher turbulence intensity. In contrast, the wall heat flux strongly depends on the imposed disc temperature, increasing considerably as the disc temperature rises from 600 K to 800 K. The results also indicate that steering-induced variations in the relative position between the duct outlet and the brake disc can noticeably affect the local cooling performance and the uniformity of heat dissipation across the rotor surface.

From an engineering perspective, the present results highlight the importance of airflow management in the design of brake cooling systems for commercial vehicles operating under sustained thermal loads. The study demonstrates that optimizing the alignment between the duct outlet and the brake assembly, while minimizing aerodynamic losses along the airflow path, can improve convective heat dissipation and reduce localized overheating during severe braking conditions such as downhill driving, repeated braking cycles, and high vehicle loads. Therefore, the proposed forced-air duct configuration may contribute to improved thermal management, enhanced component durability, and increased operational safety in commercial vehicle braking systems.

It is important to note that the present study does not consider the rotational motion of the brake disc. In real

operating conditions, disc rotation generates a centrifugal pumping effect that enhances airflow through the internal ventilation channels and increases convective heat transfer. Consequently, the cooling performance predicted in this work should be interpreted as conservative. Future research should incorporate the coupled effects of brake disc rotation and external forced airflow, as well as further aerodynamic optimization of the duct geometry under different operating conditions. Experimental validation of the numerical predictions would also be valuable to confirm the thermal and aerodynamic behavior of the proposed cooling configuration under realistic driving conditions.

REFERENCES

[1] Haddar, M.B.J., Ghorbel, A., Djemal, F., Baccar, M., Haddar, M. (2024). Heat transfer and flow analysis through a new brake disc design: A CFD approach. International Journal on Interactive Design and Manufacturing, 19(6): 4215-4224. https://doi.org/10.1007/s12008-024-02027-2

[2] Coulibaly, A., Zioui, N., Bentouba, S., Kelouwani, S., Bourouis, M. (2021). Use of thermoelectric generators to harvest energy from motor vehicle brake discs. Case Studies in Thermal Engineering, 28: 101379. https://doi.org/10.1016/j.csite.2021.101379

[3] Zhang, J., Zuo, J. (2025). Numerical thermo-mechanical modeling of tread braking systems under ultra-long downhill constant-speed conditions with coupled time-dependent heat partition coefficients. International Communications in Heat and Mass Transfer, 169: 109713. https://doi.org/10.1016/j.icheatmasstransfer.2025.109713

[4] Liu, H., He, Z., Zhang, Q., Liao, C., Xiong, K., Wang, X., Zhao, C., Mo, J. (2026). Friction interface evolution and braking performance of high-speed trains on long downhill slopes under extreme cold environment. Wear, 588: 206521. https://doi.org/10.1016/j.wear.2026.206521

[5] Cai, J., Xu, Q., Yan, J., Lin, Y., Mao, J. (2026). Effects of brake disk structure on heat dissipation and wear performance. Journal of Mechanical Science and Technology, 40(2): 1039-1051. https://doi.org/10.1007/s12206-026-0123-2

[6] Umaras, E., Barari, A., Tsuzuki, M.S.G. (2021). Heavy vehicles brake drums — An accurate evaluation on thermal loads in severe service conditions. International Journal of Automotive Technology, 22(2): 371-382. https://doi.org/10.1007/s12239-021-0035-1

[7] Belhocine, A., Wan Omar, W.Z. (2017). Computational fluid dynamics (CFD) analysis and numerical aerodynamic investigations of automotive disc brake rotor. Australian Journal of Mechanical Engineering, 16(3): 188-205. https://doi.org/10.1080/14484846.2017.1325118

[8] Bhardwaj, A. (2017). A CFD investigation of aerodynamic effects of wheel center geometry on brake cooling. In AE World Congress Experience, Detroit, Michigan, United States. https://doi.org/10.4271/2017-01-1537

[9] Li, C., Yang, H.I. (2023). Optimized shape for improved cooling of ventilated discs. Alexandria Engineering Journal, 79: 556-567. https://doi.org/10.1016/j.aej.2023.08.035

[10] Minh, C.N., Van, Q.D., Dinh, T.N., Van, Q.L. (2024). Numerical investigation of material and structural influence on transient temperature behavior in disc brakes during single-stop braking. International Journal of Heat and Technology, 42(4): 1337-1348. https://doi.org/10.18280/ijht.420424

[11] Zuo, J., Zheng, S., Wang, X. (2024). The thermo-mechanical coupling method of brake disc based on dynamic convective heat transfer. Numerical Heat Transfer, Part A: Applications, 86(20): 7344-7358. https://doi.org/10.1080/10407782.2024.2350032

[12] Cravero, C., Marsano, D. (2022). Flow and thermal analysis of a racing car braking system. Energies, 15(8): 2934. https://doi.org/10.3390/en15082934

[13] Marin, F.B., Marin, M. (2021). CFD modeling of aerodynamic car brake cooling system. The Annals of "Dunarea de Jos" University of Galati. Fascicle IX, Metallurgy and Materials Science, 44(4): 44-47. https://doi.org/10.35219/mms.2021.4.08

[14] García-León, R.A., Afanador-García, N., Gómez-Camperos, J.A. (2021). Numerical study of heat transfer and speed air flow on performance of an auto-ventilated disc brake. Fluids, 6(4): 160. https://doi.org/10.3390/fluids6040160

[15] Ravinthiran, A., Ravi Kumar, L., Srivarshani, P., Sharadha, S., Saravanan, V., Ajith Kumar, R. (2024). Design optimization of disc brake rotor. In International Conference on Trends in Automotive Parts Systems and Applications, Kuniamuthur, Coimbatore, India. https://doi.org/10.4271/2023-01-5146

[16] Orlandi, F., Coccetta, M., Meleti, S., Milani, M., Montorsi, L. (2025). A comprehensive CFD approach of a thermal analysis of a braking discs system under different design conditions. International Journal of Thermofluids, 25: 101004. https://doi.org/10.1016/j.ijft.2024.101004

[17] Ttito, D.N., Suarez, D.Q., Gutierrez, J.A., Quispe, W.B., Carpio, P.P., Arapa, C.D. (2025). Design and implementation of fog light ducts to optimize hot air recirculation and heat transfer in the Toyota Hilux. International Journal of Heat and Technology, 43(5): 1631-1643. https://doi.org/10.18280/ijht.430502

[18] Sathiyan, T.K., Vdovin, A., Johansson, S., Sebben, S. (2024). Experimental thermal analysis of brake cooling relative to mass flow of air through a ventilated brake disc. Case Studies in Thermal Engineering, 64: 105530. https://doi.org/10.1016/j.csite.2024.105530

[19] Zhang, Y., Jin, X., He, M., Wang, L., Wang, Q., Wang, L., Wu, Y. (2017). The convective heat transfer characteristics on outside surface of vehicle brake disc. International Journal of Thermal Sciences, 120: 366-376. https://doi.org/10.1016/j.ijthermalsci.2017.06.020

[20] Ciolfi, M.J., de Mello, P.E.B. (2015). Heat transfer analysis in a usual ventilated brake disc. In 12th SAE Brasil International Brake Colloquium & Engineering Display, Sao Paulo, Brazil. https://doi.org/10.4271/2015-36-0019

[21] Tirovic, M., Galindo-Lopez, C.H. (2008). Convective heat dissipation from a wheel-hub-mounted railway brake disc. Proceedings of the Institution of Mechanical Engineers, Part F: Journal of Rail and Rapid Transit, 222(4): 355-365.

https://doi.org/10.1243/09544097jrrt135

NOMENCLATURE

h	Convective heat transfer coefficient, $W \cdot m^{-2} \cdot K^{-1}$
Ma	Mach number, dimensionless
P	Pressure, Pa
ΔP	Pressure drop, Pa
q	Wall heat flux, $W \cdot m^{-2}$
Re	Reynolds Number, dimensionless
T	Temperature, K
v	Velocity, $m \cdot s^{-1}$
W	Total power dissipation, W